Molecular Pharmacology Fast Forward. Published on November 18, 2011 as doi:10.1124/mol.111.074120

MOL #74120

AC927, a σ Ligand, Blocks Methamphetamine-Induced Release of Dopamine and Generation of Reactive Oxygen Species in NG108-15 Cells

Nidhi Kaushal, Meenal Elliott, Matthew J. Robson, Anand Krishnan V. Iyer, Yon Rojanasakul, Andrew Coop and Rae R. Matsumoto

Department of Basic Pharmaceutical Sciences, School of Pharmacy, West Virginia University Health Sciences Center, Morgantown, WV 26506 USA (N.K., M.E., M.J.R., A.K.V.I., Y.R., R.R.M.); Department of Pharmaceutical Sciences, School of Pharmacy, University of Maryland, Baltimore, MD 21201, USA (A.C.)

Molecular Pharmacology Fast Forward. Published on November 18, 2011 as DOI: 10.1124/mol.111.074120
This article has not been copyedited and formatted. The final version may differ from this version.

a) Running Title: AC927 blocks METH-induced neurotoxicity in NG108-15 cells

b) Corresponding Author: Dr. Rae R. Matsumoto, West Virginia University, School of Pharmacy, P.O. Box 9500, Morgantown, WV 26506. Tel: 1-304-293-1450; Fax: 1-304-293-2576; Email: rmatsumoto@hsc.wvu.edu

c) Number of text pages: 39

Number of tables: 2

Number of figures: 6

Number of references: 40

Number of words in the abstract: 212

Number of words in the introduction: 604

Number of words in the discussion: 1385

d) Abbreviations used: AC927, N-phenethylpiperidine oxalate; ANOVA, analysis of variance; BiP, binding immunoglobulin protein; CM-H_2DCFDA, 5-(and-6)-chloromethyl-2',7'-dichlorodihydrofluorescin diacetate, acetyl ester; DAT**,** dopamine transporter; DMEM, Dulbecco's modified Eagle's medium; DMSO, dimethylsulfoxide; DTT, dithiothreitol; EDTA, ethylenediaminetetraaceticacid; ELISA, enzyme-linked immunosorbent assay; ER, endoplasmic reticulum; FITC, fluorescin isothiocyanate; FBS, fetal bovine serum; HAT, hypoxanthine-aminopterin-thymidine; H_2O_2, hydrogen peroxide; IP_3, inositol trisphosphate; METH, methamphetamine; $Na_2Cr_2O_7$, sodium bichromate; NAC, N-acetylcysteine; NaN_3, sodium azide; $Na_2S_2O_5$, sodium metabisulfite; L-NMMA, L-N^G-monomethyl arginine citrate; KCl, potassium chloride; MFI, mean fluorescence intensity; NET, norepinephrine transporter; $\cdot ONOO^-$, peroxynitrite; $^{\cdot}OH^-$, hydroxyl; $\cdot NO$, nitric oxide; $\cdot O_2^-$, superoxide; PBS, phosphate buffered saline; qRT-PCR, quantitative real time polymerase chain reaction; RFU, relative fluorescence units; RNS, reactive nitrogen species; ROS**,** reactive oxygen species; SDS, sodium dodecyl sulfate; SERT, serotonin transporter; TH, tyrosine hydroxylase

Molecular Pharmacology Fast Forward. Published on November 18, 2011 as DOI: 10.1124/mol.111.074120
This article has not been copyedited and formatted. The final version may differ from this version.

Abstract

Methamphetamine is a highly addictive psychostimulant drug of abuse that causes neurotoxicity at high or repeated dosing. Earlier studies have demonstrated the ability of the selective sigma receptor ligand AC927 (N-phenethylpiperidine oxalate) to attenuate the neurotoxic effects of methamphetamine *in vivo*. However, the precise mechanisms through which AC927 conveys its protective effects remain to be determined. Using differentiated NG108-15 cells as a model system, the effects of methamphetamine on neurotoxic endpoints and mediators like apoptosis, necrosis, generation of reactive oxygen and nitrogen species (ROS/RNS) and dopamine release were examined in the absence and presence of AC927. Methamphetamine at physiologically relevant micromolar concentrations caused apoptosis in NG108-15 cells. At higher concentrations of methamphetamine, necrotic cell death was observed. At earlier time points, methamphetamine caused ROS/RNS generation which was detected by the fluorigenic substrate CM-H_2DCFDA in a concentration and time dependent manner. N-acetylcysteine, catalase, and L-NMMA inhibited the ROS/RNS fluorescence signal induced by methamphetamine, suggesting the formation of hydrogen peroxide and reactive nitrogen species. Exposure to methamphetamine also stimulated the release of dopamine from NG108-15 cells into the culture medium. AC927 attenuated methamphetamine-induced apoptosis, necrosis, ROS/RNS generation and dopamine release in NG108-15 cells. Together, the data suggest that modulation of sigma receptors can mitigate methamphetamine-induced cytotoxicity, ROS/RNS generation, and dopamine release in cultured cells.

Molecular Pharmacology Fast Forward. Published on November 18, 2011 as DOI: 10.1124/mol.111.074120
This article has not been copyedited and formatted. The final version may differ from this version.

Introduction

Methamphetamine (METH) is a highly abused psychostimulant drug that results in neurotoxicity at high or repeated drug administration (Krasnova and Cadet, 2009). This neurotoxicity is seen as dopamine nerve terminal degeneration and apoptosis in several brain regions (Krasnova and Cadet, 2009), the mechanism of which is not completely understood. However, some of the neurotoxic cascades involved are excessive release of dopamine, oxidative/nitrosative stress, endoplasmic reticulum (ER) stress, and activation of mitochondrial death cascades (Cadet and Brannock, 1998; Krasnova and Cadet, 2009).

Among its various targets, METH interacts with sigma (σ) receptors at physiologically relevant micromolar concentrations (Han and Gu, 2006; Nguyen et al., 2005). Two subtypes of σ receptors, σ_1 and σ_2, are expressed in almost all types of mammalian cells (Guitart et al., 2004). σ_1 Receptors are highly conserved 223 amino acid membrane bound proteins (Kekuda et al., 1996). They function as chaperones at the mitochondrial-ER membrane and regulate Ca^{2+} signaling via inositol trisphosphate (IP_3) receptors (Hayashi and Su, 2007). Additionally, σ_1 receptors can undergo protein-protein interactions with several other cellular proteins such as binding immunoglobulin protein (BiP), ankyrin-B, IP_3 receptors, and dopamine D_1 receptors (Hayashi and Su, 2007; Navarro et al., 2010; Su et al., 2010). σ_1 Receptors are also capable of translocation to different subcellular compartments upon stimulation through ligand binding and changes in intracellular conditions (Hayashi and Su, 2003). In contrast, σ_2 receptors are less well characterized. However, they are elevated in immortalized cell lines and tumor cells (Vilner et al., 1995), where they have been implicated in the control of cell cycle functions (Wheeler et al., 2000), alterations in cellular Ca^{2+} levels (Vilner and Bowen, 2000), and cell death signaling involving sphingolipid products (Crawford et al., 2002).

Previous *in vivo* studies have shown that pretreatment with AC927 (N-phenethylpiperidine oxalate), a σ receptor ligand, attenuates the neurotoxic effects of METH in male, Swiss Webster mice (Matsumoto et al., 2008; Seminerio et al., 2011). The ability of

Molecular Pharmacology Fast Forward. Published on November 18, 2011 as DOI: 10.1124/mol.111.074120
This article has not been copyedited and formatted. The final version may differ from this version.

AC927 to mitigate neurotoxic cascades is consistent with the location of σ receptors in various subcellular organelles like ER, mitochondria, lysosomes, cell membrane, and nucleus (McCann et al., 1994; Zeng et al., 2007) as well as the functional roles of σ receptors in cells as described above. Nevertheless, the role of σ receptors in neurotoxicity resulting from drugs of abuse like METH remains unclear due to various limitations, including the lack of a suitable *in vitro* model system. Previous studies to understand the mechanisms of METH-induced toxicity employed either primary neuronal cultures or immortalized cell lines of neuronal origin (Cadet et al., 1997; Wu et al., 2007). In order to induce cell death/damage, millimolar concentrations of METH were required, which are rarely achieved *in vivo* (Melega et al., 2008). Therefore, a model system suitable for identifying potential mechanisms leading to neurotoxicity is needed.

In order to elucidate the cellular mechanisms of METH-induced neurotoxicity at which AC927 may intervene via σ receptors, a neuronal/glial cell culture model (neuroblastoma × glioma hybridoma, NG108-15 cells) was used in the present study. NG108-15 cells when differentiated display neurite outgrowth, electrical excitability, and express proteins with neuronal and glial properties (Ma et al., 1998). These cells have been used extensively as a sensitive cell line to study the toxic effects of various drugs and chemicals (Canete and Diogene, 2008). Additionally, NG108-15 cells have been commonly used in the literature to study the functions of σ receptors (Hayashi and Su, 2003). In the current study, the end points measured were reactive oxygen and nitrogen species (ROS/RNS) generation, dopamine release, apoptosis, and necrosis. Finally, AC927 was tested against these cytotoxic endpoints and mediators to gain insight into the mechanisms of σ-mediated neuroprotection.

Molecular Pharmacology Fast Forward. Published on November 18, 2011 as DOI: 10.1124/mol.111.074120
This article has not been copyedited and formatted. The final version may differ from this version.

Materials and Methods

Drugs and Chemicals. Phosphate buffered saline (PBS), Dulbecco's modified Eagle's medium (DMEM), penicillin-streptomycin solution, hypoxanthine-aminopterin-thymidine solution (HAT), trypsin-EDTA (0.05% trypsin; 0.43 mM EDTA), 5-(and-6)-chloromethyl-2',7'-dichlorodihydrofluorescein diacetate (CM-H_2DCFDA), dithiothreitol (DTT), and Trizol lysis reagent were obtained from Invitrogen (Carlsbad, CA). Ammonium persulfate, fetal bovine serum (FBS), dimethylsulfoxide (DMSO), methamphetamine-HCl, sodium dichromate, catalase, N-acetylcysteine (NAC), L-N^G-monomethyl arginine citrate (L-NMMA), potassium chloride (KCl), sodium azide (NaN_3), sodium bichromate ($Na_2Cr_2O_7.2H_2O$), sodium metabisulfite ($Na_2S_2O_5$), trizma base, glycine, tris-buffered saline with Tween 20, and ethylenediaminetetraaceticacid (EDTA) were obtained from Sigma–Aldrich Chemicals (St. Louis, MO). Chloroform, hydrogen peroxide (H_2O_2), hydrochloric acid (HCl), isopropanol and methanol were purchased from Fisher Scientific (Pittsburgh, PA), and polyacrylamide-bis acrylamise solution (37.5:1, 2.6%C), sodium dodecyl sulfate (SDS, 20%) and TEMED from Bio-Rad Laboratories (Hercules, CA). Permeabilization-fixation (Perm-Fix) staining buffer kit was obtained from BD Biosciences (San Jose, CA). AC927 (N-phenethylpiperidine oxalate) was synthesized in the laboratory of Dr. Andrew Coop (University of Maryland, Baltimore, MD) as previously described (Maeda et al., 2002).

Cell Line and Culture. The neuroblastoma x glioma hybridoma cell line, NG108-15 was obtained from ATCC (Rockville, MD). Cells were maintained in 25 cm^2 (T25) or 75 cm^2 (T75) culture flasks (Corning-Costar, Lowell, MA) in hi-glucose (4.5 g/l) DMEM supplemented with 10% FBS, penicillin, streptomycin, and HAT at 37^{o}C in a humidified incubator in 5% CO_2. When cells were 70% confluent in the flasks, the medium was replaced with differentiation medium (DMEM with 0.5% FBS, penicillin, streptomycin, HAT and 1% DMSO) and allowed to differentiate for an additional 2-4 days prior to harvesting for dopamine and flow cytometry assays and quantitative real-time PCR studies. For reactive oxygen species (ROS) assays, cells

Molecular Pharmacology Fast Forward. Published on November 18, 2011 as DOI: 10.1124/mol.111.074120
This article has not been copyedited and formatted. The final version may differ from this version.

were plated in 48-well CellBind tissue culture plates (Corning-Costar, Lowell, MA) in complete medium at 2.5 x 10^4 cells per well and allowed to become 80% confluent whereupon the culture medium was replaced with differentiation medium and the cells allowed to differentiate for a further 2-4 days. For apoptosis assays, cells were plated in BD Falcon black Optilux 96-well plates (BD Biosciences, San Jose, CA) coated with a mix of poly-D-lysine and mouse laminin (1 μg/cm^2 each) in complete medium at 10^4 cells per well. The medium was replaced after 24 hr with differentiation medium (DMEM with 0.5% FBS, penicillin, streptomycin, HAT and 1% DMSO) and the cells were allowed to differentiate for a further 3-4 days.

Flow Cytometry. NG108-15 cells grown and differentiated in T75 flasks were harvested, washed once with PBS containing 1% FBS, and 0.09% NaN_3. Cells were fixed and permeabilized in Perm-Fix buffer for 20 min on ice, washed with Perm-Wash buffer and incubated for 20 min with the following primary antibodies: chicken anti-σ_1 receptor antibody (aa65-78; LRRLHPGHVLPDEE) or non-specific chicken IgY (Aves Laboratories, Tigard, OR), rabbit anti-tyrosine hydroxylase antibody (AB152) or non-specific rabbit IgG antibody (12-370; Millipore Corporation, Billerica, MA) at 1:100 dilution per 10^6 cells. Cells were washed once with Perm-Wash buffer and counterstained for 20 min with the following fluorescin isothiocyanate (FITC) conjugated secondary antibodies: rabbit anti-chicken antibody or goat anti-rabbit antibody (Southern Biotechnology Associates, Birmingham, AL). Cells were washed in Perm-Wash buffer once more and resuspended in PBS containing 1% FBS and 0.09% NaN_3 and data were acquired employing FACSCaliber (Beckton Dickinson, San Jose, CA). The data were plotted and analyzed using FCS Software (De Novo Software, Ontario, Canada). The mean fluorescence intensity (MFI) of staining from multiple experiments was subjected to statistical analyses.

Real-time PCR. NG108-15 cells grown and differentiated in T25 flasks as described above were harvested, washed once with cold PBS and re-suspended in appropriate extraction buffer. Bilateral striatum samples were dissected from male Swiss Webster mice, flash frozen

Molecular Pharmacology Fast Forward. Published on November 18, 2011 as DOI: 10.1124/mol.111.074120
This article has not been copyedited and formatted. The final version may differ from this version.

and stored at -80^{o}C until later RNA isolation. RNA isolations were conducted using Trizol reagent according to manufacturer's instructions (Invitrogen, Carlsbad, CA). Quality and quantity of RNA was assessed using a spectrophotometer (Biochrom, Cambridge, England). One μg of RNA was used to synthesize cDNA, employing Superscript-H cDNA synthesis kits (Applied Biosystems, Foster City, CA), which was then used as a template for RT-PCR employing oligonucleotide primer sets specific for 18s rRNA (Hs99999901_s1), mouse DAT mRNA (Mm00438396_m1), mouse σ_1 mRNA (Mm00448086M1), mouse SERT mRNA (Mm00439391_m1), mouse NET mRNA (Mm00436661_m1), rat NET mRNA (Rn00580207_m1), mouse dopamine D_1 mRNA (Mm01353211_m1), rat dopamine D_1 mRNA (Rn03062203_s1), and Taqman RT-PCR master mix (Applied Biosystems, Foster City, CA) for 45 cycles in a Step One Plus real time PCR system. Cycles to threshold (ΔC_T) for each sample were recorded, using 18s as an endogenous control. Threshold was set at 0.2 for all genes tested. The $\Delta\Delta C_T$ method was used to calculate relative quantities of each gene in NG108-15 cells as compared to mouse or rat striatum samples.

ROS Assays. Cells grown in complete or differentiation medium were used for assays when 60-70% confluent. The culture medium was replaced with 200 μl of phenol red free medium containing 0.5% FBS and 5 μM of the fluorigenic, oxidizable dye CM-H_2DCFDA and returned to the incubator at 37^{o}C for 45-60 min. Cells were gently rinsed once with phenol red free medium, fed with 200 μl of the same medium and appropriate concentrations of METH or AC927 ranging from 0 to 300 μM. Exogenously added 100 μM H_2O_2 served as a positive control in this assay. Also included was 100 μM $Na_2Cr_2O_7$, a well-known source of carcinogenic chromium VI (O'Brien et al., 2003) which has been previously shown to induce ROS in human lung cancer cells (Azad et al., 2008). All compounds were added in replicates of 4 or 8 and the plates were returned to the incubator. In some assays, AC927 was added 15 min prior to the addition of METH, $Na_2Cr_2O_7$ or H_2O_2. Inhibitors of ROS were added at the same time as the dye

Molecular Pharmacology Fast Forward. Published on November 18, 2011 as DOI: 10.1124/mol.111.074120
This article has not been copyedited and formatted. The final version may differ from this version.

prior to the addition of METH, $Na_2Cr_2O_7$ or H_2O_2 and again after rinsing cells to remove remaining extracellular dye and prior to adding METH. At specified time points, plates were read in a Fluostar Optima fluorescence plate reader fitted with a 485/520 nm excitation/emission filter set (BMG Labtech GmbH, Offenberg, Germany). Data were obtained as relative fluorescence units (RFU) after background subtraction. In some assays, RFU for untreated controls for each assay were averaged and the values for each treated sample normalized to this average followed by statistical analyses.

Dopamine Quantitation. NG108-15 cells grown and differentiated in T75 flasks were harvested by replacing the medium with Ca^{2+}, Mg^{2+} free DPBS, centrifuged, re-suspended in differentiation medium with reduced glucose (1.5 g/l) at 3 x 10^5 cells per ml and seeded in 24 well CellBind tissue culture plates at 0.5 ml per well. After 4 hr, various concentrations of METH (0-300 µM) were added to sets of wells. KCl (50 mM) was used as a positive control for maximum dopamine release. In one set of wells, AC927 (0.3 µM) was added 15 min prior to the addition of METH or KCl. After 5 min of exposure to KCl or METH, supernatants were harvested (450 µl), centrifuged to remove cells, acidified with the addition of 1/10 volume of buffer (0.1 N HCl, 10 mM EDTA and 40 mM $Na_2S_2O_5$) and samples were stored at -20^{o}C. Dopamine was quantitated using an enzyme-linked immunosorbent assay (ELISA) kit from Rocky Mountain Diagnostics (Denver, CO) and manufacturer's protocols. Briefly, dopamine was extracted from the culture supernatants by binding to an affinity gel matrix, acetylated, eluted, and then measured using ultra sensitive competition ELISA and a standard curve of known concentrations of dopamine.

Apoptosis and Necrosis Assays. NG108-15 cells were grown and differentiated in 96-well plates. On the day of the experiment, the culture medium was replaced with 100 µl phenol red free differentiation media. The cells were pretreated with AC927 (0-30 µM), 15 min prior to treatment with various concentrations of METH (0-1 mM) for 24 hr at 37^{o}C. 20 µg/ml Hoechst

Molecular Pharmacology Fast Forward. Published on November 18, 2011 as DOI: 10.1124/mol.111.074120
This article has not been copyedited and formatted. The final version may differ from this version.

33342 stain (Invitrogen, Carlsbad, CA) and propidium iodide (Invitrogen, Carlsbad, CA) were added to the wells and the plate was incubated at room temperature for 10 min. After the incubation step, the plate was placed under the microscope with UV light and 2-3 pictures/well were taken using Leica Application Suite: Imaging software (Leica Microsystems Inc., Buffalo Grove, IL). Cells which were bright blue stained and displayed fragmented nuclei were counted as apoptotic and cells that were red were counted as necrotic. The percentage of apoptotic and necrotic cells were calculated using an Image J cell counter (NIH, Bethesda, MD).

Statistical Analyses. Statistical analyses of data included t-tests and analysis of variance (ANOVA) with appropriate post-hoc tests employing GraphPad Prism 4 (GraphPad Software, San Diego, CA).

Molecular Pharmacology Fast Forward. Published on November 18, 2011 as DOI: 10.1124/mol.111.074120
This article has not been copyedited and formatted. The final version may differ from this version.

Results

Differentiated NG108-15 Cells Express σ_1 Receptors and Tyrosine Hydroxylase.

Fig. 1A shows representative histograms from flow cytometric detection of the σ_1 receptor and tyrosine hydroxylase (TH) in fixed and permeabilised NG108-15 cells. Staining employing chicken anti-σ_1 and rabbit anti-TH antibodies was found in single peaks with mean fluorescence intensities (MFI) of 38.24 ± 2.52 and 39.60 ± 2.87, respectively, while control antibodies chicken IgY and rabbit IgG detected peaks with MFI of 3.35 ± 0.08 and 3.30 ± 0.09, respectively, and represented background staining. Statistical analysis using unpaired t-tests of results obtained in six separate experiments (Fig. 1B) confirmed a significant shift in MFI for antigen-specific staining over background (t = 13.80, p < 0.0001 for σ_1 vs. control IgY and t = 12.63, p < 0.0001 for TH vs. control IgG).

Differentiated NG108-15 Cells Express DAT, SERT, NET and Dopamine D_1 Receptor mRNA.

Table 1 depicts mRNA expression levels of DAT, SERT, NET, dopamine D_1 receptors, as well as σ_1 receptors in differentiated NG108-15 cells and rat or mouse striatum. ΔC_T values, as well as the gene fold change ratio of NG108-15 cell/respective striatum samples are included. Unpaired two-tailed t-tests were used to compare levels of mRNA between mouse or rat striatum and differentiated NG108-15 cells. There was a significant difference in mRNA expression levels of DAT (t = 16.95, p < 0.0001), σ_1 receptors (t = 3.07, p < 0.01), SERT (t = 5.98, p < 0.0001), and dopamine D_1 receptors (mouse: t = 47.20, p < 0.0001; rat: t = 34.73, p < 0.0001). However, NET was expressed in a similar quantity in both NG108-15 cells and rat striatum (t = 0.87, ns). Mouse NET was found not to be expressed in differentiated NG108-15 cells.

METH Generates Reactive Oxygen/Nitrogen Species in Differentiated NG108-15 Cells.

As shown in Fig. 2A, CM-H_2DCFDA detected exogenously added H_2O_2 within 10 min (168.91 ± 6.95 % of untreated control) and up to 60 min (176.69 ± 7.10 % of control). Low levels

Molecular Pharmacology Fast Forward. Published on November 18, 2011 as DOI: 10.1124/mol.111.074120
This article has not been copyedited and formatted. The final version may differ from this version.

of ROS were also induced in NG108-15 cells by $Na_2Cr_2O_7$ starting at 10 min; ROS in this sample increased dramatically 4 hr after treatment (140.10 ± 8.60 % of control) and continued to increase up to 24 hr reaching 223.70 ± 21.92 % of that in untreated control cells.

All tested concentrations of METH except the lowest (0.1 μM) induced the production of ROS capable of oxidizing CM-H_2DCFDA significantly above background levels within 10 min of exposure, with 3 μM inducing the highest levels (201.97 ± 9.97 % of control, Table 2). The difference between METH-induced ROS and basal ROS in NG108-15 cells diminished beyond 60 min, while ROS continued to accumulate in cells treated with $Na_2Cr_2O_7$ up to 24 hr. Statistical analysis of the data obtained from 10 to 60 min employing two-way repeated measures ANOVA and Bonferroni's post-hoc tests further established that concentrations of METH capable of reproducibly inducing the strongest and sustained ROS responses were 1 μM ($p < 0.001$), 3 μM ($p < 0.001$), and 300 μM ($p < 0.001$) concentrations at 10, 20, 30 and 60 min (Table 2).

As shown in Figure 2B, CM-H_2DCFDA detected exogenously added H_2O_2 within 10 min (146.69 ± 4.97 % of control) and ROS generated by $Na_2Cr_2O_7$ in NG108-15 cells, which peaked at 24 hr (242.06 ± 11.56 % of control). In contrast, all tested concentrations of AC927 from 0 to 300 μM failed to induce ROS significantly higher than that in untreated control cells. Statistical analyses of the data employing two-way repeated measures ANOVA showed a significant effect of AC927 and positive control treatment ($F[9,900] = 75.37$, $p < 0.0001$), time ($F[6,900] = 28.36$, $p < 0.0001$) and AC927 and positive control treatment × time interaction ($F[54,900] = 60.50$, $p < 0.0001$). Bonferroni's post-hoc tests revealed that none of the tested concentrations of AC927 were able to induce elevation of ROS above background levels, while ROS was detected in cells treated with H_2O_2 (10 min: $t = 11.26$, $p < 0.001$; 20 min: $t = 14.14$, $p < 0.001$; 30 min: $t = 14.50$, $p < 0.001$; 60 min: $t = 11.47$, $p < 0.001$; 240 min: $t = 3.03$, $p < 0.05$ and 480 min: $t = 3.00$, $p < 0.05$) and $Na_2Cr_2O_7$ (240 min: $t = 7.01$, $p < 0.001$; 480 min: $t = 16.52$, $p < 0.001$ and 1440 min: $t = 34.24$, $p < 0.001$). Interestingly, AC927 at 0.3 μM led to a reduction in basal ROS in

Molecular Pharmacology Fast Forward. Published on November 18, 2011 as DOI: 10.1124/mol.111.074120
This article has not been copyedited and formatted. The final version may differ from this version.

NG108-15 cells, the reduction becoming statistically significant at 240 min (t = 3.78, p < 0.01), 480 min (t = 2.87, p < 0.05) and up to 1440 min (t = 4.38, p < 0.001).

As shown in Fig. 3A, ROS detectable by CM-H_2DCFDA induced in NG108-15 cells by 0.1 to 3 μM METH was completely inhibited in the presence of the common antioxidant and radical scavenger NAC as seen within 20 min of addition of the drug, confirming that the assay was indeed detecting ROS (Fig. 3A). One-way ANOVA showed that the inhibition was significant (F[13,99] = 95.57, p < 0.0001). Bonferroni's post-hoc tests with pairwise comparisons showed that NAC induced a significant decrease in ROS for all tested concentrations of METH (t = 11.96 to 13.64, p < 0.001 for all concentrations). Significant inhibition of radical generation persisted up to 4 hr after addition of METH, at which time the experiment was terminated. Interestingly, NAC also reduced the ROS detectable in untreated control cells (t = 7.97, p < 0.001).

The presence of catalase in the assay medium (10000 units per ml) inhibited ROS induced by 1 and 3 μM METH and was detected by CM-H_2DCFDA within 20 min of addition of the drug (Fig. 3B). One-way ANOVA confirmed that the inhibition was significant (F[11,91] = 7.74, p < 0.0001). Bonferroni's post-hoc tests with pairwise comparisons placed significant differences at both 1μM (t = 3.17, p < 0.05) and 3 μM (t = 3.20, p < 0.05) of METH.

Finally, the increase in ROS in NG108-15 cells induced by 1 and 3 μM METH was also significantly inhibited in the presence of L-NMMA; data shown were obtained 20 min after addition of the drug (Fig. 3C, F[13,83] = 28.41, p < 0.0001, one-way ANOVA). Bonferroni's post-hoc tests and pairwise comparisons revealed significant changes at both 1 μM (t = 4.20, p < 0.001) and 3 μM (t = 4.78, p < 0.001) of METH.

AC927 Attenuates METH-Induced ROS/RNS Generation in Differentiated NG108-15 Cells. As shown in Figure 4, METH caused a significant increase in ROS/RNS generation (F[10,79] = 13.84, p < 0.0001). Post-hoc Dunnett's tests showed that all the concentrations of

Molecular Pharmacology Fast Forward. Published on November 18, 2011 as DOI: 10.1124/mol.111.074120
This article has not been copyedited and formatted. The final version may differ from this version.

METH except 30 μM showed significant ROS/RNS generation: 0.1 μM (q = 3.62, p < 0.01), 0.3 μM (q = 3.42, p < 0.01), 1 μM (q = 4.44, p < 0.01), 3 μM (q = 8.30, p < 0.01), 10 μM (q = 3.63, p < 0.01), 100 μM (q = 3.42, p < 0.01) and 300 μM (q = 7.39, p < 0.01). 0.3 μM AC927 attenuated the production of reactive radicals induced by METH, reducing them to levels observed in untreated control cells for all tested concentrations of METH; data shown here were obtained 20 min following stimulation with METH. Two-way ANOVA showed a significant effect of AC927 pretreatment (F[1,138] = 98.44, p < 0.0001), METH or positive control treatment (F[10,138] = 15.63, p < 0.0001) and AC927 pretreatment × METH or positive control treatment interaction (F[10,138] = 2.39, p < 0.05). Bonferroni's post-hoc tests showed that AC927 attenuated ROS/RNS generated by the following METH concentrations: 0.1 μM (t = 3.28, p < 0.05), 0.3 μM (t = 3.16, p < 0.05), 1 μM (t = 3.52, p < 0.01), 3 μM (t = 7.16, p < 0.001), 10 μM (t = 3.99, p < 0.01), 30 μM (t = 3.14, p < 0.05), 100 μM (t = 3.39, p < 0.05) and 300 μM (t = 3.84, p < 0.01). As expected, AC927 did not inhibit the oxidation of the dye by exogenously added H_2O_2 at 20 min (t = 1.39, ns) or at later time points. It also failed to significantly inhibit the small amount of ROS generated by $Na_2Cr_2O_7$ at this time point (t = 0.99, ns). However, at later time points, AC927 inhibited ROS induction by $Na_2Cr_2O_7$ as seen at 4 hr (t = 4.05, p < 0.001) and 24 hr (t = 7.73, p < 0.001).

AC927 Attenuates METH-Induced Dopamine Release in Differentiated NG108-15 Cells. As shown in Fig. 5, in untreated cells, 0.0 to 41.85 pg of dopamine was detected. In contrast, when cells were treated with KCl, 268.30 to 389.62 pg of dopamine was detected in the culture supernatant 5 min following exposure.

Dopamine release was induced by all four concentrations of METH ranging from 0.3 to 300 μM, with 3 μM METH inducing maximum release with 204.75 to 413.12 pg per 1.5 x 10^5 cells, compared to that in untreated control cells (F[5,23] = 8.87, p < 0.0005). In cells treated with 0.3, 30 and 300 μM of METH, mean values for dopamine levels ranged from 153.00 ±

Molecular Pharmacology Fast Forward. Published on November 18, 2011 as DOI: 10.1124/mol.111.074120
This article has not been copyedited and formatted. The final version may differ from this version.

46.60 to 165.50 ± 27.81 pg per 1.5 x 10^5 cells. Levels of dopamine released in response to 0.3, 3 and 300 μM of METH were significantly above those in untreated controls (q = 2.77, p < 0.05; q = 5.32, p < 0.01 and q = 2.76, p < 0.05, respectively, Dunnett's multiple comparisons tests).

In cells exposed to 0.3 μM AC927 for 5 min, dopamine levels were not significantly different from those in untreated controls (Fig. 5). Pre-exposure of cells to 0.3 μM AC927 for 15 min prior to stimulation with METH prevented the release of dopamine (mean values ranging from 8.84 to 32.33 pg per 1.5 x 10^5 cells). The attenuation of dopamine release by AC927 was statistically significant as judged by one-way ANOVA (F[11,41] = 13.96, p < 0.0001) and Bonferroni's post-hoc tests with pairwise comparisons, for the 0.3 μM (t = 3.19, p < 0.05) and 3 μM (t = 5.58, p < 0.001) concentrations of METH. Pretreatment of cells with AC927 did not, however, block the release of dopamine in cells treated with KCl (t = 0.23, ns).

AC927 Prevents METH-Induced Apoptosis and Necrosis in Differentiated NG108-15 Cells. The apoptotic effects of various concentrations of METH (0-1 mM) on NG108-15 cells over a period of 24 hr are shown in Fig. 6A. One-way ANOVA showed that METH caused a significant and concentration dependent increase in the percentage of apoptotic cells (F[7,187] = 37.21, p < 0.0001). Post-hoc analysis employing Dunnett's tests showed that the following concentrations of METH caused significant increases in apoptosis when compared with controls: 3 μM (q = 2.87, p < 0.05), 10 μM (q = 3.74, p < 0.01), 100 μM (q = 5.99, p < 0.001), 300 μM (q = 7.73, p < 0.001), and 1000 μM (q = 13.68, p < 0.001).

AC927 pretreatment significantly attenuated the apoptotic effects of METH. Two-way ANOVA showed a significant effect of METH treatment (F[6,392] = 37.82, p < 0.0001), AC927 pretreatment (F[3,392] = 55.94, p < 0.0001) and METH treatment × AC927 pretreatment interaction (F[18,392] = 5.41, p < 0.0001). Post-hoc Bonferroni's tests showed that AC927 (0.3, 3 and 30 μM) attenuated the apoptotic effects of METH. AC927 (0.3 μM) attenuated the apoptotic effects of the following concentrations of METH: 3 μM (t = 3.34, p < 0.01), 10 μM (t =

Molecular Pharmacology Fast Forward. Published on November 18, 2011 as DOI: 10.1124/mol.111.074120
This article has not been copyedited and formatted. The final version may differ from this version.

3.70, $p < 0.01$), 100 μM ($t = 5.05$, $p < 0.001$), 300 μM ($t = 5.85$, $p < 0.001$), and 1000 μM ($t = 9.80$, $p < 0.001$). AC927 (3 μM) prevented the apoptotic effects of the following concentrations of METH: 10 μM ($t = 3.52$, $p < 0.01$), 100 μM ($t = 3.45$, $p < 0.01$), 300 μM ($t = 5.67$, $p < 0.001$), and 1000 μM ($t = 8.84$, $p < 0.001$). AC927 (30 μM) attenuated the apoptotic effects of the following concentrations of METH: 100 μM ($t = 3.20$, $p < 0.05$), 300 μM ($t = 3.00$, $p < 0.05$), and 1000 μM ($t = 7.82$, $p < 0.001$).

The necrotic effects of various concentrations of METH (0-1 mM) on NG108-15 cells over a period of 24 hr are shown in Fig. 6B. One-way ANOVA showed that METH caused a significant and concentration dependent increase in the percentage of necrotic cells ($F[7,187] = 7.35$, $p < 0.0001$). Post-hoc analysis employing Dunnett's tests showed that the following concentrations of METH caused significant increases in necrosis when compared with no treatment controls: 300 μM ($q = 3.82$, $p < 0.01$) and 1000 μM ($q = 5.88$, $p < 0.01$).

AC927 pretreatment significantly attenuated the necrotic effects of METH. Two-way ANOVA showed a significant effect of METH treatment ($F[6,392] = 8.32$, $p < 0.0001$) and AC927 pretreatment ($F[3,392] = 17.14$, $p < 0.0001$). Post-hoc Bonferroni's tests showed that the following concentrations of AC927 attenuated the necrotic effects of METH (300 and 1000 μM): 0.3 μM, $t = 4.33$, $p < 0.001$ and $t = 4.26$, $p < 0.001$; 3 μM, $t = 3.30$, $p < 0.01$ and $t = 3.91$, $p < 0.001$; 30 μM, $t = 3.29$, $p < 0.01$ and $t = 2.87$, $p < 0.05$.

Molecular Pharmacology Fast Forward. Published on November 18, 2011 as DOI: 10.1124/mol.111.074120
This article has not been copyedited and formatted. The final version may differ from this version.

Discussion

This study showed that METH causes apoptosis in differentiated NG108-15 cells at physiologically relevant micromolar concentrations and can cause necrosis at higher concentrations. At earlier time points, ROS/RNS generation and release of dopamine were also observed. AC927, a σ receptor ligand, attenuated the apoptotic and necrotic cell death as well as the neurotoxicity mediators. The implications of these findings are further discussed below.

In the first part of the study, differentiated NG108-15 cells were confirmed to express various receptors and transporters through which METH mediates its effects: σ_1 and dopamine D_1 receptors; dopamine, serotonin and norepinephrine transporters; and the synthetic enzyme tyrosine hydroxylase. Extensive studies in the literature have also corroborated the presence of σ receptors in NG108-15 cells (Su et al., 2010; Vilner et al., 1995). Previous studies have also demonstrated the production of dopamine in these differentiated catecholaminergic cells (Ghahary et al., 1989). Collectively, the presence of tyrosine hydroxylase, monoamine transporters, and D_1 receptors suggests a functional dopaminergic neurotransmitter system in these cells. Although the levels of DAT are low in the NG108-15 cell line, higher levels of SERT can compensate by functional reuptake of dopamine released into the synapse (Schmidt and Lovenberg, 1985).

One of the key mediators of METH's neurotoxicity is ROS/RNS generation, which can occur through multiple mechanisms including excessive dopamine release, microglial activation, glutamate release, and mitochondrial dysfunction (Krasnova and Cadet, 2009). Excessive generation of ROS/RNS can injure neurons and surrounding cells via direct oxidative damage to cellular components such as lipids, proteins, and DNA, or by causing ER stress and activation of mitochondrial death cascades, ultimately leading to nerve terminal degeneration or cell death (Krasnova and Cadet, 2009). This study demonstrated that METH generates ROS/RNS in the NG108-15 model system. All tested concentrations of METH ranging from 0.1 to 300 μM induced the production of ROS/RNS within 10 min of exposure. High and stable ROS/RNS

Molecular Pharmacology Fast Forward. Published on November 18, 2011 as DOI: 10.1124/mol.111.074120
This article has not been copyedited and formatted. The final version may differ from this version.

levels were detected at 20 min and up to 60 min after exposure of NG108-15 cells to METH. After the first hour, the levels of ROS/RNS decreased, indicating that the cells may shift to the production of radicals not detected by CM-H_2DCFDA. Alternately, in METH-treated cells, endogenous peroxidases as well as antioxidants such as glutathione may be rapidly recruited after the first hour to scavenge H_2O_2 and $\cdot ONOO^-$ radicals.

At the early time point (20 min) that gave consistent and robust ROS/RNS signals following METH administration, the antioxidant NAC reduced the signal indicating that the fluorescent probe CM-H_2DCFDA was detecting ROS/RNS. In addition, catalase and L-NMMA also decreased the METH-induced signal indicating that H_2O_2 and NO species were being generated. This result is consistent with the ability of METH to generate H_2O_2 and NO species from various sources including dopamine oxidation and glutamate-induced NOS activation (Krasnova and Cadet, 2009). It is also interesting to note that the dose response of METH-induced reactive species generation did not follow a classical sigmoidal pattern, displaying highest radical generation at the 3 μM concentration. This pattern of results is most likely due to multiple mechanisms and sources of METH's ROS/RNS generation (Krasnova and Cadet, 2009).

AC927 pretreatment attenuated the ROS/RNS generated by METH. This effect of AC927 does not seem to be a general antioxidant effect because AC927 did not prevent the H_2O_2-mediated ROS signal or reduce the basal cellular ROS/RNS signal. However, at the 4 hr time point onwards, AC927 (0.3 μM) attenuated the basal cellular ROS/RNS levels as well as the ROS signal produced by $Na_2Cr_2O_7$. $Na_2Cr_2O_7$ generates $\cdot O_2^-$, H_2O_2 and $\cdot OH^-$ in the cell (Azad et al., 2008). In combination with NO, $\cdot O_2^-$ can produce $\cdot ONOO^-$ in the cell. The ability of AC927 to attenuate the ROS signal produced by $Na_2Cr_2O_7$ and not H_2O_2 is most likely due to increased levels of cellular antioxidant/antioxidant enzymes like superoxide dismutase which can reduce superoxide levels in the cell, or decreased levels of enzymes like NOS which can generate NO leading to the production of $\cdot ONOO^-$. Since this effect of AC927 is observed after 4 hr and not

Molecular Pharmacology Fast Forward. Published on November 18, 2011 as DOI: 10.1124/mol.111.074120
This article has not been copyedited and formatted. The final version may differ from this version.

before, it suggests the induction of cellular antioxidants or a decrease in pro-oxidant/nitrosative stress enzymes, rather than the effect of generalized intrinsic antioxidant activity.

Corroborating with this interpretation, several studies in the literature demonstrate the ability of σ receptors to modulate cellular ROS/RNS generation and antioxidant systems. Previous studies in tumor cells have shown that σ_2 receptor activation causes ROS generation (Ostenfeld et al., 2005). σ_1 Receptors are also involved in oxidative stress-mediated toxicities like ischemic stroke and have been shown to provide protective effects (Schetz et al., 2007). σ Receptors also play a regulatory role in the redox state of the cell, and can modulate cellular NOS enzyme activity (Tsai et al., 2009; Yang et al., 2010). In addition to modulating the cellular redox system, σ receptors can also regulate other systems that are involved in ROS/RNS generation by METH. First, σ receptors can regulate glutamate release through NMDA receptors which in turn causes nNOS activation and nitrosative stress (DeCoster et al., 1995). Second, σ receptors can modulate microglial activation through Ca^{2+} dependent mechanisms, which can contribute to the release of inflammatory cytokines and ROS/RNS generation (Hall et al., 2009). Third, σ receptors can regulate the release of dopamine which in turn undergoes autooxidation and is a major cause of METH's ROS generation (Derbez et al., 2002; Gonzalez-Alvear and Werling, 1994).

Although additional studies are needed to identify the specific mechanism(s) through which AC927 reduces the generation of METH-induced ROS/RNS, the studies conducted herein suggest that the modulation of dopamine release may be an important contributor. AC927 attenuates METH-induced dopamine release from the NG108-15 cells, with peak release observed at the 3 μM concentration of METH which is consistent with the peak observed in the ROS assay. Moreover, AC927 pretreatment prevented the dopamine release caused by METH, but not the non-specific dopamine release caused by K^+-mediated hyperpolarization. This is consistent with the role of σ receptors in regulating DAT function and dopamine release in several *in vivo* and *in vitro* studies, including the involvement of Ca^{2+}-

Molecular Pharmacology Fast Forward. Published on November 18, 2011 as DOI: 10.1124/mol.111.074120
This article has not been copyedited and formatted. The final version may differ from this version.

dependent and protein kinase C-mediated mechanisms (Booth and Baldessarini, 1991; Derbez et al., 2002). In addition to modulation of DAT function by σ receptors at lower concentrations, AC927 at higher concentrations may also act in part as a DAT blocker in NG108-15 cells. The affinity of AC927 for DAT is 2939 ± 452 nM (Matsumoto et al., 2008). In addition, unpublished data suggests that AC927 at 1 μM can significantly attenuate dopamine uptake from rat synaptosomes (Werling, personal communication).

METH also caused apoptosis and necrosis in NG108-15 cells. Oxidative and nitrosative stress in the cell can lead to the activation of pro death pathways like mitochondrial release of cytochrome c, and/or caspase 3 activation which ultimately leads to apoptotic or necrotic cell death (Higuchi et al., 1998). AC927 significantly attenuated both the apoptotic and necrotic cell death which is consistent with the role of σ receptors in cell death mechanisms (Bowen, 2000; Marrazzo et al., 2011). Furthermore, the protective effects of AC927 observed in NG108-15 cells is complementary and consistent with the neuroprotection observed in earlier *in vivo* studies (Matsumoto et al., 2008; Seminerio et al., 2011). Moreover, in tumor cells, AC927 has been shown to prevent apoptosis caused by σ_2 receptor agonists, further underscoring an important role of σ receptors in cell death mechanisms (Marrazzo et al., 2011).

Apart from σ receptors, D_1 receptor antagonism can also protect against the apoptotic effects of METH (Jayanthi et al., 2005). Recent studies have shown that σ_1 and D_1 receptors heteromerize in cells, which has implications for the downstream effects of psychostimulants including the activation of adenyl cyclase and MAPK pathways (Navarro et al., 2010). Therefore, AC927 may potentially modulate the σ_1 and D_1 interaction and mitigate the toxic effects of METH.

In summary, our data demonstrates that METH can cause apoptosis and necrosis in an *in vitro* system representative of a differentiated neuronal cell, which mechanistically involves dopamine release and induction of reactive oxygen/nitrogen radicals. Additionally, a synthetic σ ligand, AC927, can attenuate the cytotoxic effects of METH and contributing neurotoxic

Molecular Pharmacology Fast Forward. Published on November 18, 2011 as DOI: 10.1124/mol.111.074120
This article has not been copyedited and formatted. The final version may differ from this version.

mechanisms. Future studies will be directed towards the elucidation of the downstream neurotoxic pathways activated after ROS/RNS generation in differentiated NG108-15 cells. Also, the individual contributions of the two subtypes of σ receptors will have to be discerned, as better tools are developed.

Molecular Pharmacology Fast Forward. Published on November 18, 2011 as DOI: 10.1124/mol.111.074120
This article has not been copyedited and formatted. The final version may differ from this version.

Acknowledgments

We appreciate the expert technical advice of Dr. Kathy Brundage in the WVU flow cytometry core facility. We also acknowledge Suidjit Luanpitopone for helping us set up the apoptosis and necrosis assays.

Authorship Contributions

Participated in research design: Kaushal, Elliott, Robson, Iyer, Rojanasakul, Matsumoto

Conducted experiments: Kaushal, Elliott, Robson

Contributed new reagents or analytical tools: Coop

Performed data analysis: Kaushal, Elliott, Robson, Matsumoto

Wrote or contributed to the writing of the manuscript: Kaushal, Elliott, Robson, Iyer, Rojanasakul, Matsumoto

Molecular Pharmacology Fast Forward. Published on November 18, 2011 as DOI: 10.1124/mol.111.074120
This article has not been copyedited and formatted. The final version may differ from this version.

References

Azad N, Iyer AK, Manosroi A, Wang L and Rojanasakul Y (2008) Superoxide-mediated proteasomal degradation of Bcl-2 determines cell susceptibility to Cr(VI)-induced apoptosis. *Carcinogenesis* 29(8):1538-1545.

Booth RG and Baldessarini RJ (1991) (+)-6,7-benzomorphan sigma ligands stimulate dopamine synthesis in rat corpus striatum tissue. *Brain Res* 557(1-2):349-352.

Bowen WD (2000) Sigma receptors: recent advances and new clinical potentials. *Pharm Acta Helv* 74(2-3):211-218.

Cadet JL and Brannock C (1998) Free radicals and the pathobiology of brain dopamine systems. *Neurochem Int* 32(2):117-131.

Cadet JL, Ordonez SV and Ordonez JV (1997) Methamphetamine induces apoptosis in immortalized neural cells: protection by the proto-oncogene, bcl-2. *Synapse* 25(2):176-184.

Canete E and Diogene J (2008) Comparative study of the use of neuroblastoma cells (Neuro-2a) and neuroblastomaxglioma hybrid cells (NG108-15) for the toxic effect quantification of marine toxins. *Toxicon* 52(4):541-550.

Crawford KW, Coop A and Bowen WD (2002) σ_2 Receptors regulate changes in sphingolipid levels in breast tumor cells. *Eur J Pharmacol* 443(1-3):207-209.

DeCoster MA, Klette KL, Knight ES and Tortella FC (1995) Sigma receptor-mediated neuroprotection against glutamate toxicity in primary rat neuronal cultures. *Brain Res* 671(1):45-53.

Derbez AE, Mody RM and Werling LL (2002) σ_2-receptor regulation of dopamine transporter via activation of protein kinase C. *J Pharmacol Exp Ther* 301(1):306-314.

Ghahary A, Vriend J and Cheng KW (1989) Modification of the indolamine content in neuroblastoma x glioma hybrid NG108-15 cells upon induced differentiation. *Cell Mol Neurobiol* 9(3):343-355.

Gonzalez-Alvear GM and Werling LL (1994) Regulation of [^{3}H]dopamine release from rat striatal slices by sigma receptor ligands. *J Pharmacol Exp Ther* 271(1):212-219.

Guitart X, Codony X and Monroy X (2004) Sigma receptors: biology and therapeutic potential. *Psychopharmacology (Berl)* 174(3):301-319.

Hall AA, Herrera Y, Ajmo CT, Jr., Cuevas J and Pennypacker KR (2009) Sigma receptors suppress multiple aspects of microglial activation. *Glia* 57(7):744-754.

Han DD and Gu HH (2006) Comparison of the monoamine transporters from human and mouse in their sensitivities to psychostimulant drugs. *BMC Pharmacol* 6:6.

Hayashi T and Su TP (2003) Intracellular dynamics of sigma-1 receptors (σ_1 binding sites) in NG108-15 cells. *J Pharmacol Exp Ther* 306(2):726-733.

Hayashi T and Su TP (2007) Sigma-1 receptor chaperones at the ER-mitochondrion interface regulate Ca^{2+} signaling and cell survival. *Cell* 131(3):596-610.

Higuchi M, Honda T, Proske RJ and Yeh ET (1998) Regulation of reactive oxygen species-induced apoptosis and necrosis by caspase 3-like proteases. *Oncogene* 17(21):2753-2760.

Jayanthi S, Deng X, Ladenheim B, McCoy MT, Cluster A, Cai NS and Cadet JL (2005) Calcineurin/NFAT-induced up-regulation of the Fas ligand/Fas death pathway is involved in methamphetamine-induced neuronal apoptosis. *Proc Natl Acad Sci U S A* 102(3):868-873.

Kekuda R, Prasad PD, Fei YJ, Leibach FH and Ganapathy V (1996) Cloning and functional expression of the human type 1 sigma receptor (hSigmaR1). *Biochem Biophys Res Commun* 229(2):553-558.

Krasnova IN and Cadet JL (2009) Methamphetamine toxicity and messengers of death. *Brain Res Rev* 60(2):379-407.

Ma W, Pancrazio JJ, Coulombe M, Dumm J, Sathanoori R, Barker JL, Kowtha VC, Stenger DA and Hickman JJ (1998) Neuronal and glial epitopes and transmitter-synthesizing enzymes appear in parallel with membrane excitability during neuroblastoma x glioma hybrid differentiation. *Brain Res Dev Brain Res* 106(1-2):155-163.

Marrazzo A, Fiorito J, Zappala L, Prezzavento O, Ronsisvalle S, Pasquinucci L, Scoto GM, Bernardini R and Ronsisvalle G (2011) Antiproliferative activity of phenylbutyrate ester of haloperidol metabolite II [(+/-)-MRJF4] in prostate cancer cells. *Eur J Med Chem* 46(1):433-438.

Matsumoto RR, Shaikh J, Wilson LL, Vedam S and Coop A (2008) Attenuation of methamphetamine-induced effects through the antagonism of sigma (σ) receptors: Evidence from in vivo and in vitro studies. *Eur Neuropsychopharmacol* 18(12):871-881.

McCann DJ, Weissman AD and Su TP (1994) Sigma-1 and sigma-2 sites in rat brain: comparison of regional, ontogenetic, and subcellular patterns. *Synapse* 17(3):182-189.

Melega WP, Jorgensen MJ, Lacan G, Way BM, Pham J, Morton G, Cho AK and Fairbanks LA (2008) Long-term methamphetamine administration in the vervet monkey models aspects of a human exposure: brain neurotoxicity and behavioral profiles. *Neuropsychopharmacology* 33(6):1441-1452.

Navarro G, Moreno E, Aymerich M, Marcellino D, McCormick PJ, Mallol J, Cortes A, Casado V, Canela EI, Ortiz J, Fuxe K, Lluis C, Ferre S and Franco R (2010) Direct involvement of sigma-1 receptors in the dopamine D1 receptor-mediated effects of cocaine. *Proc Natl Acad Sci U S A* 107(43):18676-18681.

Nguyen EC, McCracken KA, Liu Y, Pouw B and Matsumoto RR (2005) Involvement of sigma (σ) receptors in the acute actions of methamphetamine: receptor binding and behavioral studies. *Neuropharmacology* 49(5):638-645.

O'Brien TJ, Ceryak S and Patierno SR (2003) Complexities of chromium carcinogenesis: role of cellular response, repair and recovery mechanisms. *Mutat Res* 533(1-2):3-36.

Ostenfeld MS, Fehrenbacher N, Hoyer-Hansen M, Thomsen C, Farkas T and Jaattela M (2005) Effective tumor cell death by sigma-2 receptor ligand siramesine involves lysosomal leakage and oxidative stress. *Cancer Res* 65(19):8975-8983.

Schetz JA, Perez E, Liu R, Chen S, Lee I and Simpkins JW (2007) A prototypical sigma-1 receptor antagonist protects against brain ischemia. *Brain Res* 1181:1-9.

Schmidt CJ and Lovenberg W (1985) In vitro demonstration of dopamine uptake by neostriatal serotonergic neurons of the rat. *Neurosci Lett* 59(1):9-14.

Seminerio MJ, Kaushal N, Shaikh J, Huber JD, Coop A and Matsumoto RR (2011) Sigma (σ) receptor ligand, AC927 (N-phenethylpiperidine oxalate), attenuates methamphetamine-induced hyperthermia and serotonin damage in mice. *Pharmacol Biochem Behav* 98(1):12-20.

Su TP, Hayashi T, Maurice T, Buch S and Ruoho AE (2010) The sigma-1 receptor chaperone as an inter-organelle signaling modulator. *Trends Pharmacol Sci* 31(12):557-566.

Tsai SY, Hayashi T, Mori T and Su TP (2009) Sigma-1 receptor chaperones and diseases. *Cent Nerv Syst Agents Med Chem* 9(3):184-189.

Vilner BJ and Bowen WD (2000) Modulation of cellular calcium by sigma-2 receptors: release from intracellular stores in human SK-N-SH neuroblastoma cells. *J Pharmacol Exp Ther* 292(3):900-911.

Vilner BJ, John CS and Bowen WD (1995) Sigma-1 and sigma-2 receptors are expressed in a wide variety of human and rodent tumor cell lines. *Cancer Res* 55(2):408-413.

Wheeler KT, Wang LM, Wallen CA, Childers SR, Cline JM, Keng PC and Mach RH (2000) Sigma-2 receptors as a biomarker of proliferation in solid tumours. *Br J Cancer* 82(6):1223-1232.

Wu CW, Ping YH, Yen JC, Chang CY, Wang SF, Yeh CL, Chi CW and Lee HC (2007) Enhanced oxidative stress and aberrant mitochondrial biogenesis in human neuroblastoma SH-SY5Y cells during methamphetamine induced apoptosis. *Toxicol Appl Pharmacol* 220(3):243-251.

Yang ZJ, Carter EL, Torbey MT, Martin LJ and Koehler RC (2010) Sigma receptor ligand 4-phenyl-1-(4-phenylbutyl)-piperidine modulates neuronal nitric oxide synthase/postsynaptic density-95 coupling mechanisms and protects against neonatal ischemic degeneration of striatal neurons. *Exp Neurol* 221(1):166-174.

Zeng C, Vangveravong S, Xu J, Chang KC, Hotchkiss RS, Wheeler KT, Shen D, Zhuang ZP, Kung HF and Mach RH (2007) Subcellular localization of sigma-2 receptors in breast cancer cells using two-photon and confocal microscopy. *Cancer Res* 67(14):6708-6716.

Molecular Pharmacology Fast Forward. Published on November 18, 2011 as DOI: 10.1124/mol.111.074120
This article has not been copyedited and formatted. The final version may differ from this version.

Footnotes

a) This work was supported by the National Institutes of Health National Institute on Drug Abuse [Grant DA 013978].

b) Portions of this work were previously presented in abstract form at the Society for Neuroscience annual meeting, November 2010.

c) Person to receive reprint requests: Rae R. Matsumoto, West Virginia University, School of Pharmacy, P.O. Box 9500, Morgantown, WV 26506, email: rmatsumoto@hsc.wvu.edu

d) Current address of Anand Krishnan V. Iyer: Hampton University, School of Pharmacy, Hampton, VA, 23668, USA

Molecular Pharmacology Fast Forward. Published on November 18, 2011 as DOI: 10.1124/mol.111.074120
This article has not been copyedited and formatted. The final version may differ from this version.

Legends for Figures

Fig. 1. NG108-15 cells express σ_1 receptors and tyrosine hydroxylase (TH). A representative histogram from six independent experiments is shown (A). NG108-15 cells were fixed and permeabilized and stained and analyzed as described in the materials and methods. Histograms as follows: control chicken IgY (dotted black), chicken anti-σ_1 (solid black), control rabbit IgG (dotted grey), and rabbit anti-TH (solid grey) antibodies. FL1H (x-axis), fluorescence channel height; counts (y-axis), number of events detected for the corresponding fluorescence channel. Values for mean fluorescent intensities for all four stains from six separate experiments are plotted against the staining reagent (B).

Fig. 2. ROS induced in NG108-15 cells following exposure to methamphetamine (METH) or AC927. The production of ROS capable of oxidizing CM-H_2DCFDA was conducted as described in the materials and methods in NG108-15 cells following exposure to 100 μM H_2O_2, 100 μM $Na_2Cr_2O_7$ (Cr), or 0 to 300 μM METH (A), or 0 to 300 μM AC927 (B). Relative fluorescence units (rfu) from five (A) or two (B) separate experiments obtained at each indicated time point are shown; data were normalized to the mean rfu for untreated cells to obtain percent control values (n = 8/experiment) ± SEM. **p* < 0.05, ***p* < 0.01, ****p* < 0.001 vs. control treatment.

Fig. 3. Inhibition of ROS production in NG108-15 cells by N-acetylcysteine (NAC), catalase and L-N^G-monomethyl arginine (L-NMMA). Inhibition of ROS following exposure to 0 to 3 μM methamphetamine (METH) or 100 μM H_2O_2 was determined in the absence (solid bars) or presence (cross hatched bars) of 10 mM NAC (A), 10,000 units catalase (B) or 20 mM L-NMMA (C) 20 min following exposure to METH. Data represent averages of relative fluorescence units (rfu) from two separate experiments (n = 4/experiment) ± SEM. Significant differences are

Molecular Pharmacology Fast Forward. Published on November 18, 2011 as DOI: 10.1124/mol.111.074120
This article has not been copyedited and formatted. The final version may differ from this version.

noted, *$p < 0.05$, **$p < 0.01$ (control vs. METH treated) and #$p < 0.05$, ###$p < 0.001$ (METH alone vs. METH with ROS inhibitor).

Fig. 4. Inhibition of methamphetamine (METH)-induced ROS generation in NG108-15 cells by AC927. The production of ROS capable of oxidizing CM-H_2DCFDA was assessed in differentiated NG108-15 cells in the presence of 0 to 300 μM METH, 100 μM H_2O_2 or 100 μM $Na_2Cr_2O_7$ (Cr) in the absence (solid bars) or presence (cross hatched bars) of 0.3 μM AC927 as described in the methods. Data represent averages of relative fluorescence units (rfu) from two different experiments (n = 8/experiment) obtained 20 min after addition of drug ± SEM. Significant differences are noted as **$p < 0.01$ (control vs. METH treated) and #$p < 0.05$, ##$p < 0.01$, ###$p < 0.001$ (METH alone vs. METH with AC927).

Fig. 5. Release of dopamine in response to methamphetamine (METH) from NG108-15 cells. Supernatants harvested from NG108-15 cells cultured in the presence or absence of METH and/or AC927 (x-axis) and quantitated as described in the materials and methods are represented as pg dopamine per 1.5 x 10^5 cells in 500 μl of medium. Data represent means from four (METH or KCl alone) or three (METH with AC927) independent experiments ± SEM. Significant differences are noted as follows, *$p < 0.05$, **$p < 0.01$ (control vs. METH or KCl treated) and #$p < 0.05$, ###$p < 0.001$ (METH alone vs. METH with AC927).

Fig. 6. AC927 protects against methamphetamine (METH)-induced apoptosis (A) and necrosis (B). NG108-15 cells were pretreated with AC927 (0-30 μM) prior to exposure to METH (0-1 mM) for 24 hr. After 24 hr, the wells were incubated with Hoechst 33342 and propidium iodide stains (20 μg/ml each) to obtain percentages of apoptotic and necrotic cells. Data represent means from two separate experiments (n = 3/experiment) ± SEM. Significant differences are indicated

Molecular Pharmacology Fast Forward. Published on November 18, 2011 as DOI: 10.1124/mol.111.074120
This article has not been copyedited and formatted. The final version may differ from this version.

by *$p < 0.05$, **$p < 0.01$, ***$p < 0.001$ (control vs. METH treated); #$p < 0.05$, ##$p < 0.01$, ###$p < 0.001$ (METH alone vs. METH with AC927).

Molecular Pharmacology Fast Forward. Published on November 18, 2011 as DOI: 10.1124/mol.111.074120
This article has not been copyedited and formatted. The final version may differ from this version.

Table 1

mRNA expression levels of receptors and transporters in differentiated NG108-15 cells

Gene	TaqMan Probe	NG108-15 ΔC_T	Mouse Striatum ΔC_T	Rat Striatum ΔC_T	Gene Fold Change Ratio
mDAT (Slc6a3)	Mm00438396_m1	29.41 ± 0.21***	25.01 ± 0.11	ND	0.050
Sigma-1	Mm00448086_m1	16.89 ± 0.19**	17.74 ± 0.19	ND	1.760
mSERT (Slc6a4)	Mm00439391_m1	25.30 ± 0.17***	26.90 ± 0.22	ND	2.953
mNET (Slc6a2)	Mm00436661_m1	NP	ND	ND	
rNET (Slc6a2)	Rn00580207_m1	28.71 ± 0.18	ND	29.02 ± 0.32	1.144
mD1R	Mm01353211_m1	27.05 ± 0.18***	15.34 ± 0.14	ND	0.00031
rD1R	Rn03062203_s1	28.40 ± 0.36***	ND	12.81 ± 0.27	0.00002

qRT-PCR analysis of expression levels of mRNA for dopamine transporters (DAT), serotonin transporters (SERT), norepinephrine transporters (NET), dopamine D_1 receptors, as well as σ_1 receptors in NG108-15 cells as compared to either rat or mouse striatum. There were significant differences in mRNA expression levels of DAT, σ_1, SERT, and dopamine D_1 receptors; however mRNA for NET were expressed in a similar quantity in both NG108-15 cells and rat striatum. Mouse NET was not expressed in NG108-15 cells. Data shown represents ΔC_T for each respective gene in NG108-15 cells and mouse or rat bilateral striatum samples as compared to 18s endogenous control. Data is represented as mean ± SEM. $^{**}p < 0.01$, $^{***}p < 0.0001$, unpaired two tailed t-test. Gene fold changes were calculated using the $\Delta\Delta C_T$ method and

Molecular Pharmacology Fast Forward. Published on November 18, 2011 as DOI: 10.1124/mol.111.074120
This article has not been copyedited and formatted. The final version may differ from this version.

NG108-15/either rat or mouse striatum ratios calculated from these values. ND = not determined, NP = not present.

Molecular Pharmacology Fast Forward. Published on November 18, 2011 as DOI: 10.1124/mol.111.074120
This article has not been copyedited and formatted. The final version may differ from this version.

Table 2

Induction of ROS in NG108-15 cells by physiological concentrations of METH

METH (μM)	10 min	20 min	30 min	60 min
0	100.09 ± 5.14	100.05 ± 4.24	100.03 ± 3.26	100.00 ± 2.75
0.1	118.06 ± 4.01	116.22 ± 3.49	110.72 ± 2.89	109.53 ± 2.57
0.3	141.84 ± 9.61***	130.81 ± 7.22**	126.28 ± 5.64*	123.41 ± 6.69*
1	161.28 ± 8.71***	148.56 ± 5.81***	140.78 ± 5.40***	133.94 ± 5.74***
3	201.97 ± 9.97***	177.34 ± 8.04***	167.56 ± 5.18***	147.41 ± 5.10***
10	131.22 ± 8.48**	109.03 ± 3.65	113.03 ± 3.91	107.63 ± 2.86
30	134 ± 11.82***	115.81 ± 4.47	121.03 ± 4.79	115.06 ± 3.77
100	156.09 ± 8.82***	130.38 ± 6.12**	127.25 ± 6.34**	118.38 ± 4.62
300	176.38 ± 11.67***	146.59 ± 7.27***	151.44 ± 8.53***	132.94 ± 5.80***
H_2O_2 (100 μM)	168.91 ± 6.95***	166.34 ± 5.41***	164.63 ± 4.60***	176.69 ± 7.12***
Cr (100 μM)	130.53 ± 5.86**	123.34 ± 3.72*	128.47 ± 4.70**	132.28 ± 5.10**

NG108-15 cells were cultured and assayed as described in the materials and methods. Relative fluorescence units for each experimental point (each concentration of METH at distinct time points: 10, 20, 30 and 60 min) were obtained. Values for untreated cells (0 μM METH, n=32) for each assay plate were averaged and set at 100. Values for experimental points were converted to percent of untreated control for each assay plate. Data shown are means of percent control values ± SEM (n=8/experiment) from four separate experiments. Two-way repeated measures ANOVA of percent control values with Bonferroni's post-hoc tests permitted a comparison of the effect of time on each of the METH concentrations tested. Significant differences are noted by *$p < 0.05$, **$p < 0.01$ and ***$p < 0.001$. H_2O_2 and Cr served as positive controls.

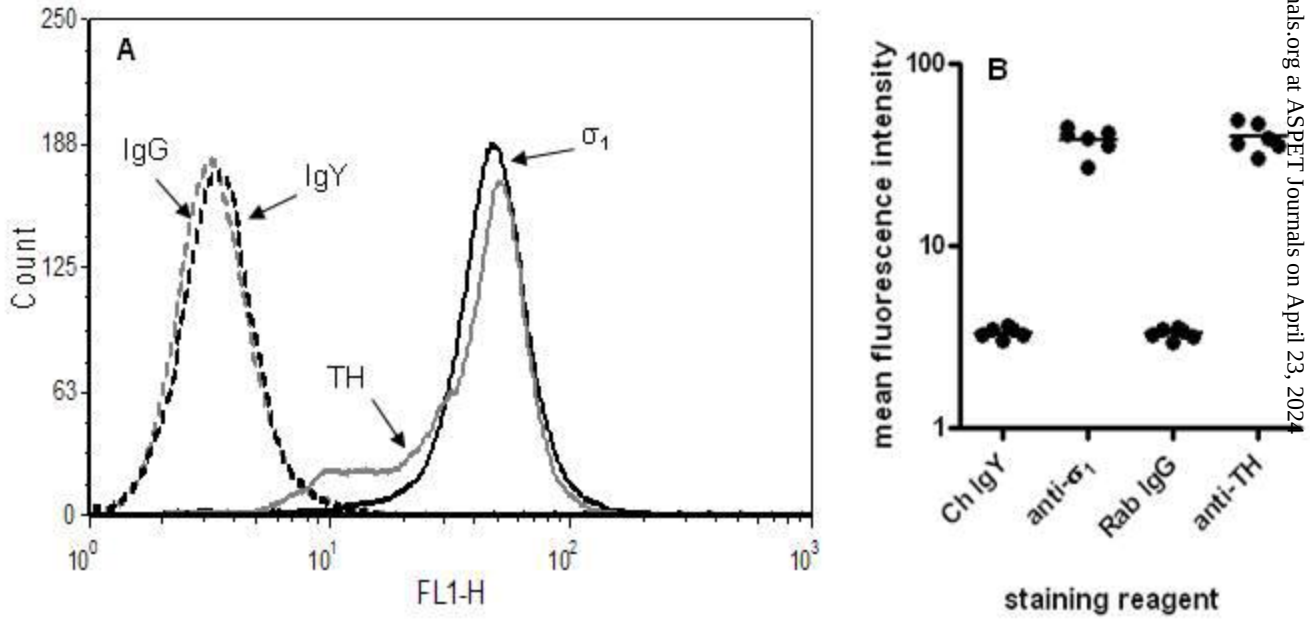

Figure 1

Molecular Pharmacology Fast Forward. Published on November 18, 2011 as DOI: 10.1124
This article has not been copyedited and formatted. The final version may differ from

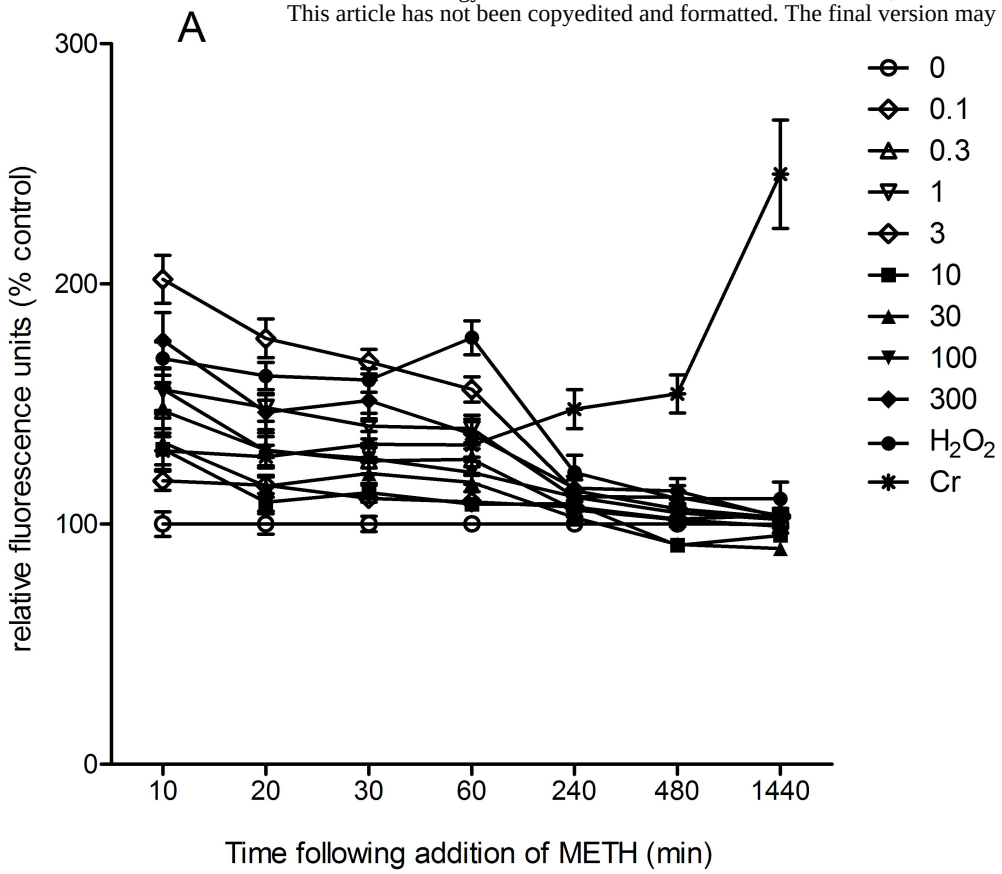

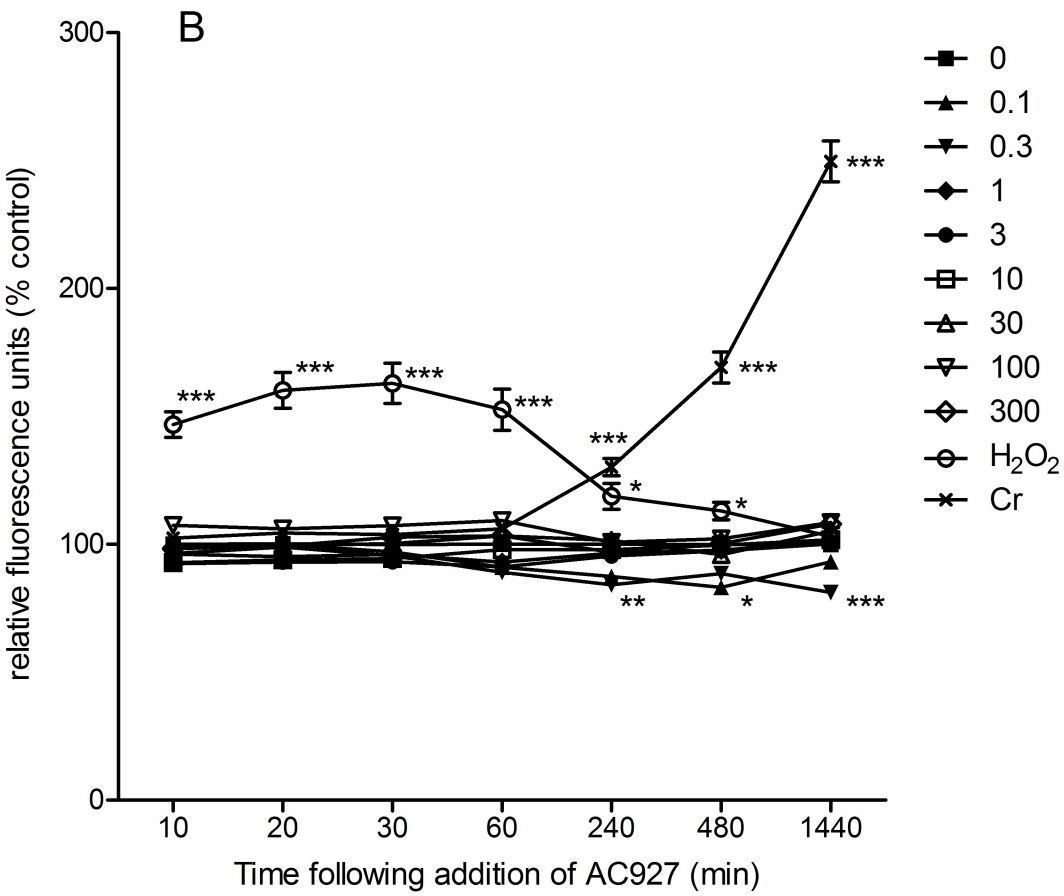

Figure 2

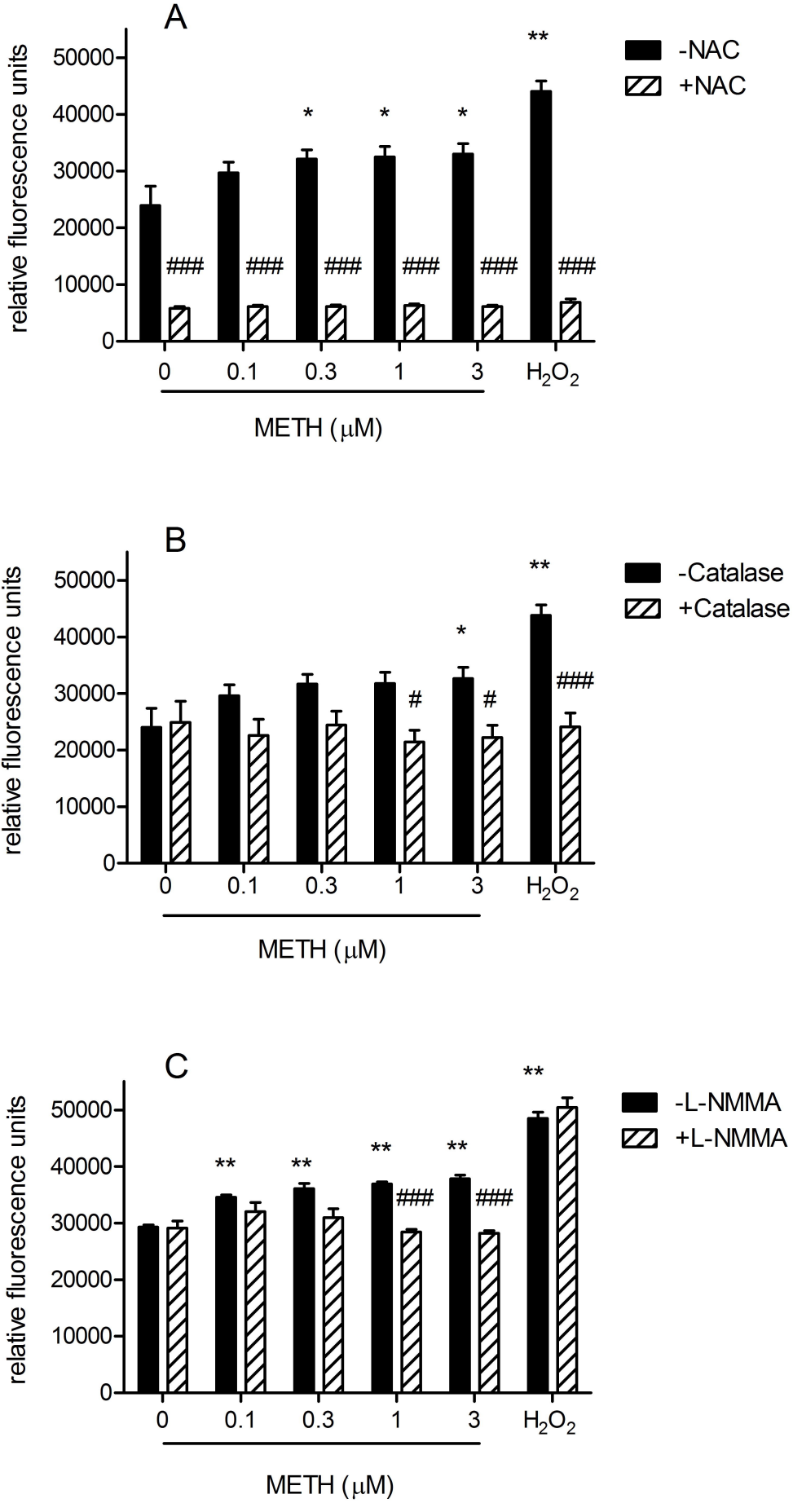

Figure 3

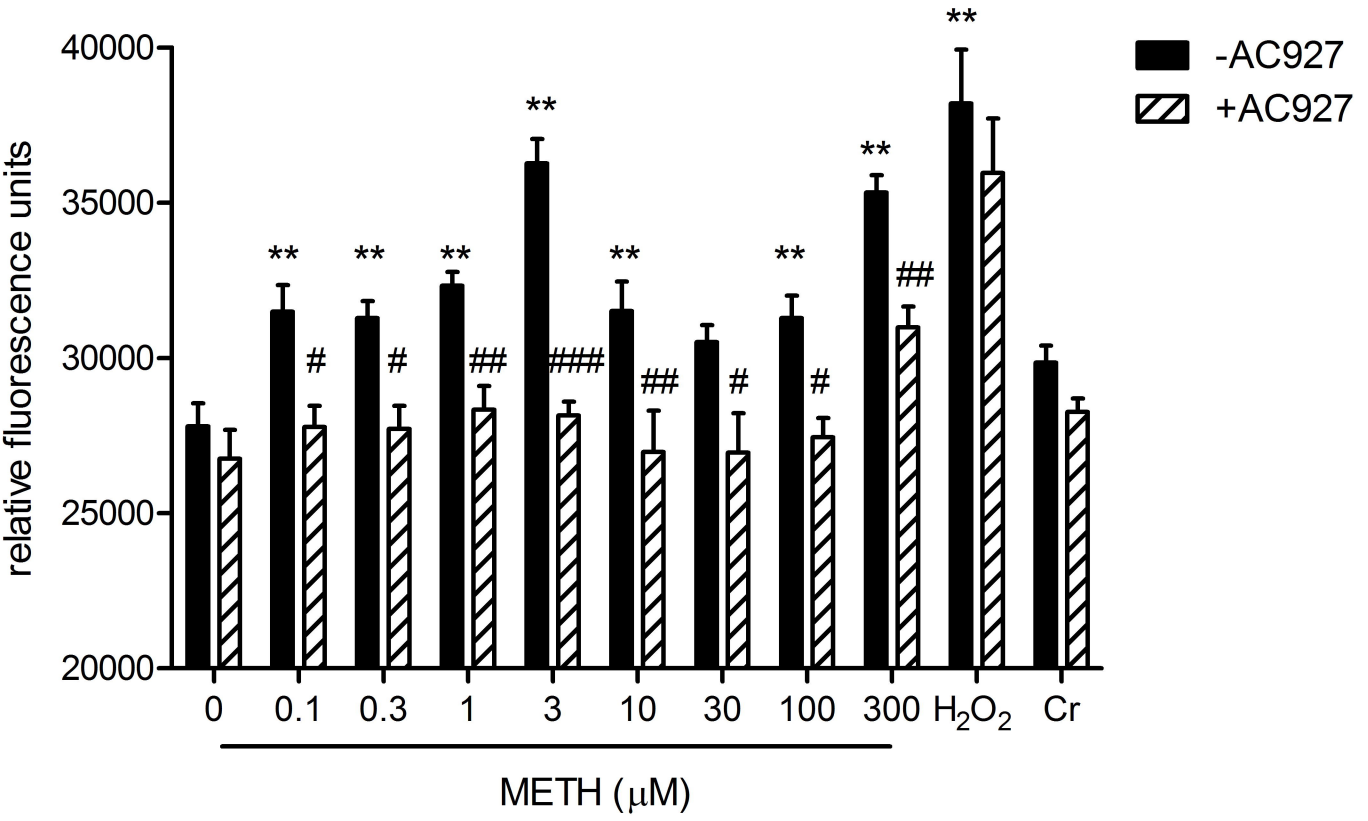
40000
35000
30000
25000
20000
relative fluorescence units
-AC927
+AC927
**
#
##
###
0
0.1
0.3
1
3
10
30
100
300
H2O2
Cr
METH (μM)

Figure 4

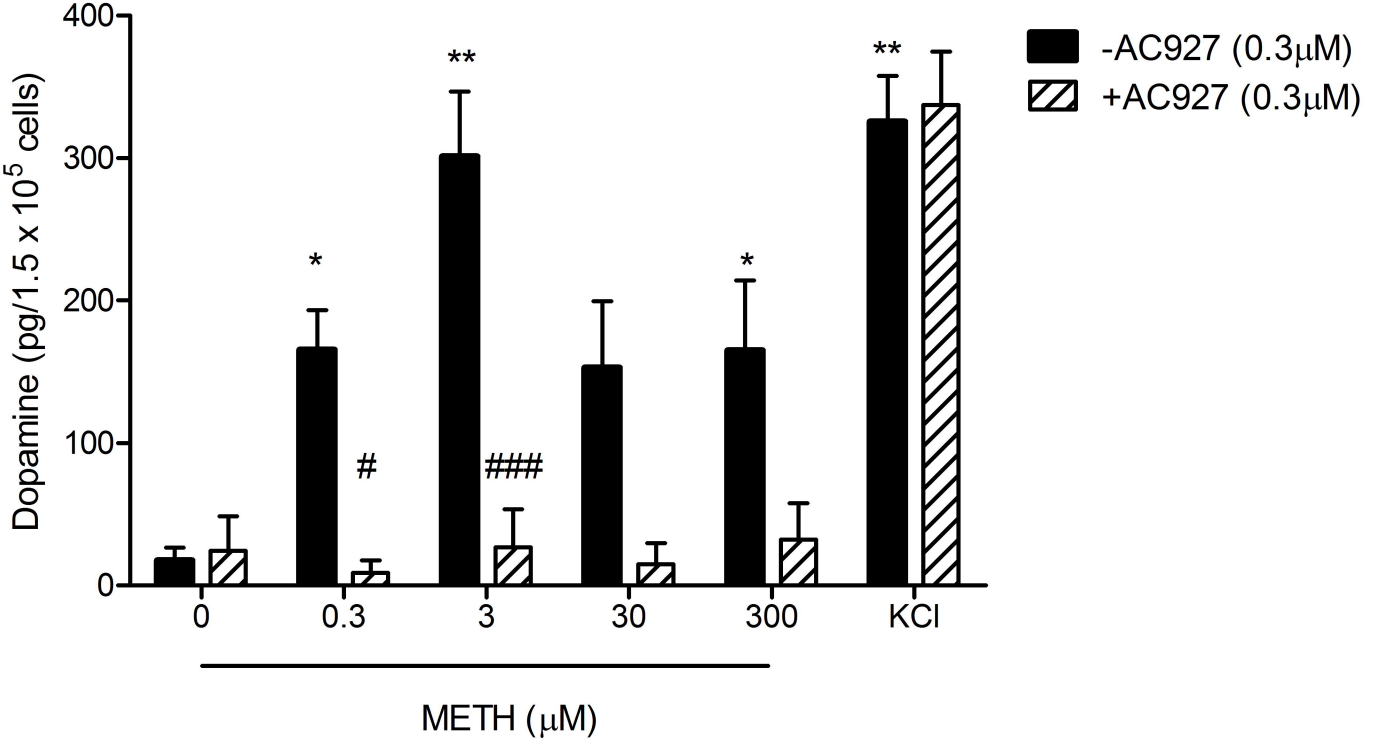
400
300
200
100
0
Dopamine (pg/1.5 x 10^5 cells)
*
**
**
*
#
###
0
0.3
3
30
300
KCl
METH (μM)
-AC927 (0.3μM)
+AC927 (0.3μM)

Figure 5

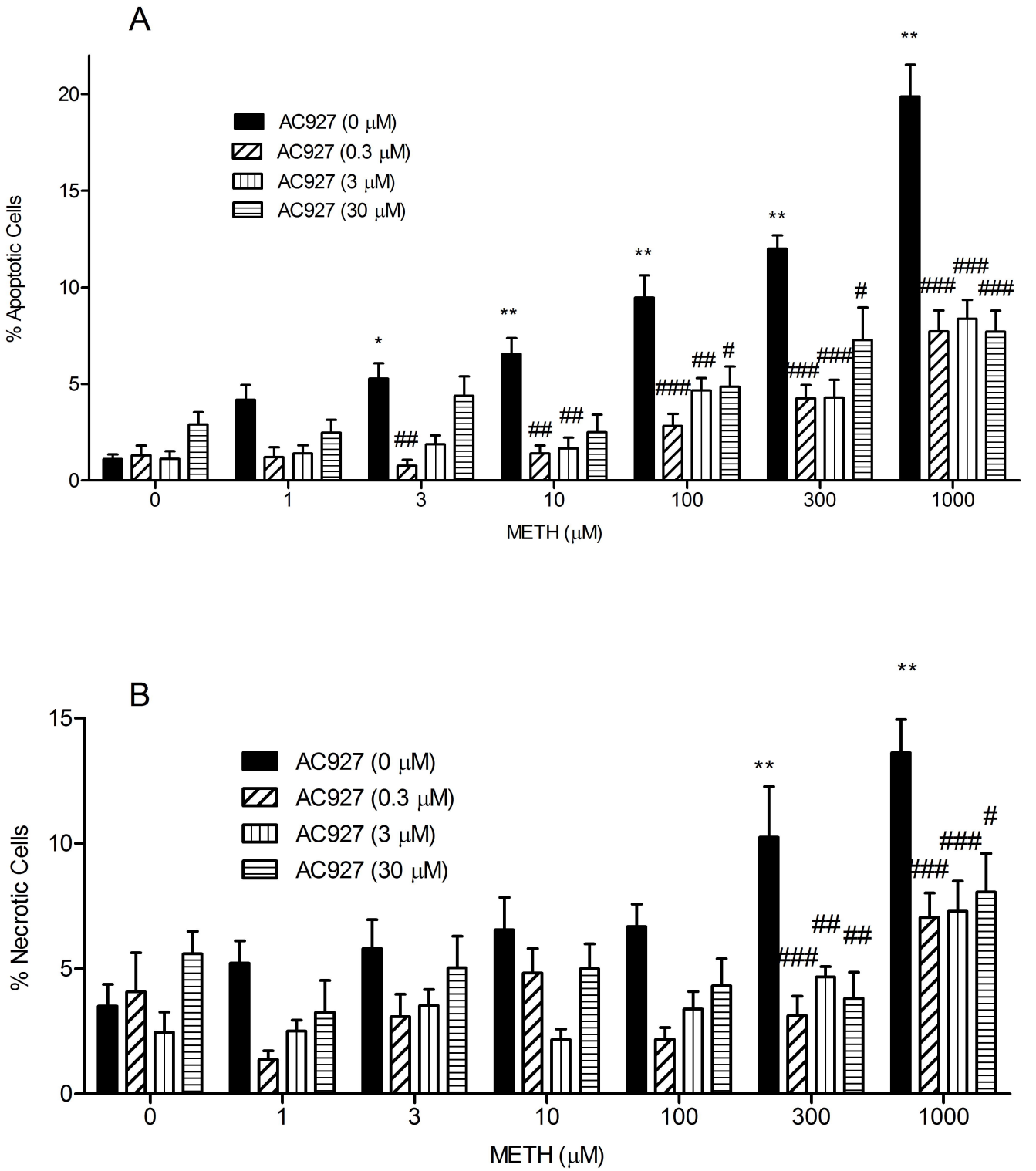
A
% Apoptotic Cells
AC927 (0 μM)
AC927 (0.3 μM)
AC927 (3 μM)
AC927 (30 μM)
METH (μM)
B
% Necrotic Cells
AC927 (0 μM)
AC927 (0.3 μM)
AC927 (3 μM)
AC927 (30 μM)
METH (μM)

Figure 6